Electronic Supplementary Material (ESI) for Journal of Materials Chemistry A.
This journal is © The Royal Society of Chemistry 2018

Electronic Supplementary Material (ESI) for Journal of Materials Chemistry A.
This journal is © The Royal Society of Chemistry 2018

Electronic Supplementary Information

Improved Conversion Efficiency of 10% for Solid-State Dye Sensitized Solar Cells Utilizing P-type Semiconducting CuI and Multi-Dye Consisting of Novel Porphyrin dimer and Organic Dyes

Naohiko Kato,*[a] Shinya Moribe,[a] Masahito Shiozawa,[a] Ryo Suzuki,[a] Kazuo Higuchi,[a]
Akira Suzuki,[b] Mareedu Sreenivasu,[b] Katsuya Tsuchimoto,[b]
Koji Tatematsu,[c] Katsuyoshi Mizumoto,[c] Shoichi Doi,[c] and Tatsuo Toyoda[c]

[a] Toyota Central Research and Development Laboratories, Inc., Nagakute-shi, Aichi 480-1192, Japan
[b] AISIN Cosmos R&D Co.,Ltd., Kariya-shi, Aichi 448-8650, Japan
[c] AISIN SEIKI Co., Ltd., Kariya-shi, Aichi 448-8650, Japan

Corresponding authors:
E-mail:e0957@mosk.tytlabs.co.jp

Relationship between the conversion efficiency and durability of liquid electrolyte DSCs

Figure S1 summarizes conversion efficiency and estimated outdoor durability of liquid electrolyte DSCs previously reported. To improve the durability, more viscous electrolytes are used, resulting in lower conversion efficiency.

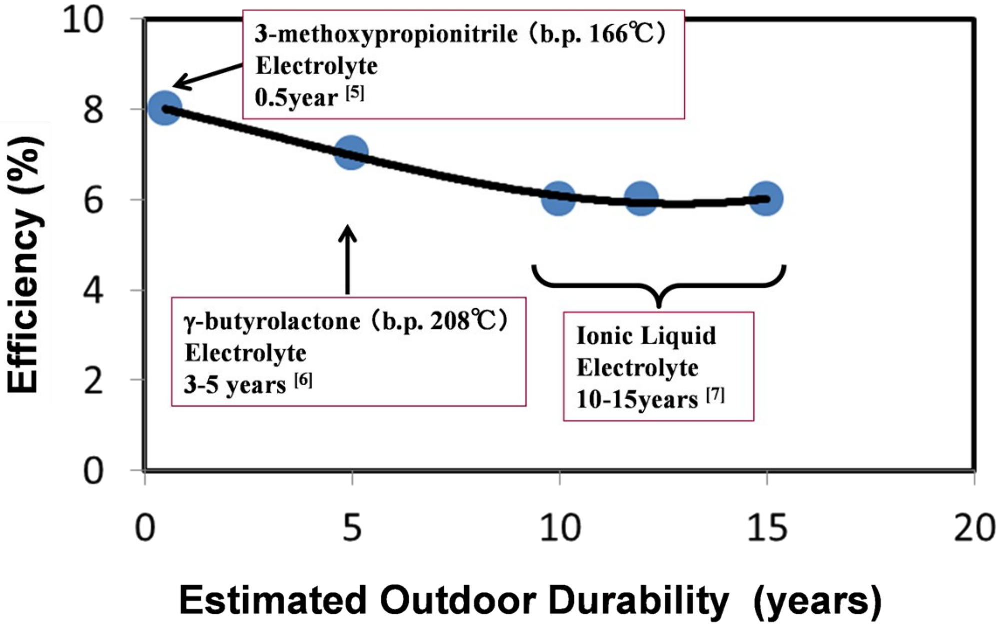

Fig. S1 Conversion efficiency and estimated outdoor durability of liquid electrolyte DSCs.

Injection process of solid-state CuI into TiO_2 electrodes

Solid-state CuI was injected into the dye-adsorbed porous TiO_2 electrodes by dropping a CuI solution (158 mM of CuI and 13.6 mM of 1-ethyl-3-methylimidazoliumthiocyanate in acetonitrile) followed by evaporation of the solvent.[1-3] The porous TiO_2 electrode on the TCO glass was put on a hot plate at 60°C. Dropping of the CuI solution of 10 µL was repeated 50 times. After the dropping process, the CuI/TiO_2 layer was covered with a thick (around 5 µm) CuI layer, as shown in Fig. S2.

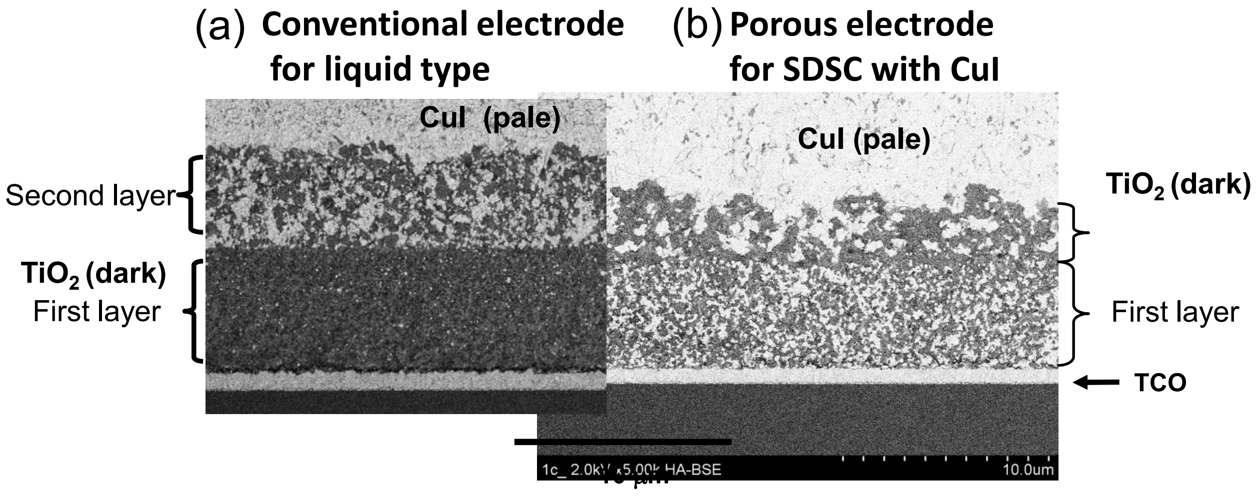

Fig. S2 SEM back-scattered electron images of the cross sections of the SDSCs consisting of double-layered TiO_2 electrodes filled with CuI. (a) 20/400 nm TiO_2 particles, (b) 35–400 (size-distributed)/400 nm TiO_2 particles.

Synthesis of the porphyrin dimer dye (DIPDAB2)

The synthesis scheme of the new porphyrin dimer dye is illustrated in Fig. S3. Both the compounds **1&2** were synthesized by several steps previously reported.[4,5] Deprotection of the silyl group in the compound **1** with tetra-butyl ammonium fluoride (TBAF) was carried out to obtain meso acetylene proton of the compound **1A**. The biporphyrin compound **3** was synthesized by Sonogashira coupling of the compound **1A** and compound **2** (Br-OC8-Porphyrin-Tips) using $Pd_2(dba)_3$ and $AsPh_3$ catalysts. Finally **DIPDAB2** was synthesized by deprotection of the silyl group in the compound **3** with TBAF and subsequent Sonogashira coupling with benzoic acid. All the steps were carried out under argon atmosphere and monitored using pre-coated TLC plates (0.20 mm with fluorescent indicator UV254). Commercially available dehydrated solvents were distilled prior to use. CH_2Cl_2 and THF were dehydrated using CaH_2 and sodium metal/benzophenone, respectively, followed by distillation immediately before use. Other commercially available reagents were used as delivered. The products were purified using silica gel columns (Merck, 100-200 Mesh ASTM), and confirmed to be the target structures by elemental analysis, ^{1}H NMR, FT-IR, and mass spectroscopy. ^{1}H NMR spectra were recorded using a JEOL - 400MHz (Varian spectrometer). FT-IR (KBr Pellet, JASCO FTIR-4100) and MALDI-TOF-MS (SHIMADZU, LC-2010EV spectrometer, operating in the positive ion detection mode) spectra were recorded using the indicated instruments. UV-vis measurements (JASCO V-630, spectrophotometer) were applied to characterize the absorption range of **DIPDAB2**. The results for the compound **3** depicted in Figs S4 and S5, and those in Figs S6, S7 and S8 for **DIPDAB2** clearly show the formation of the target structures.

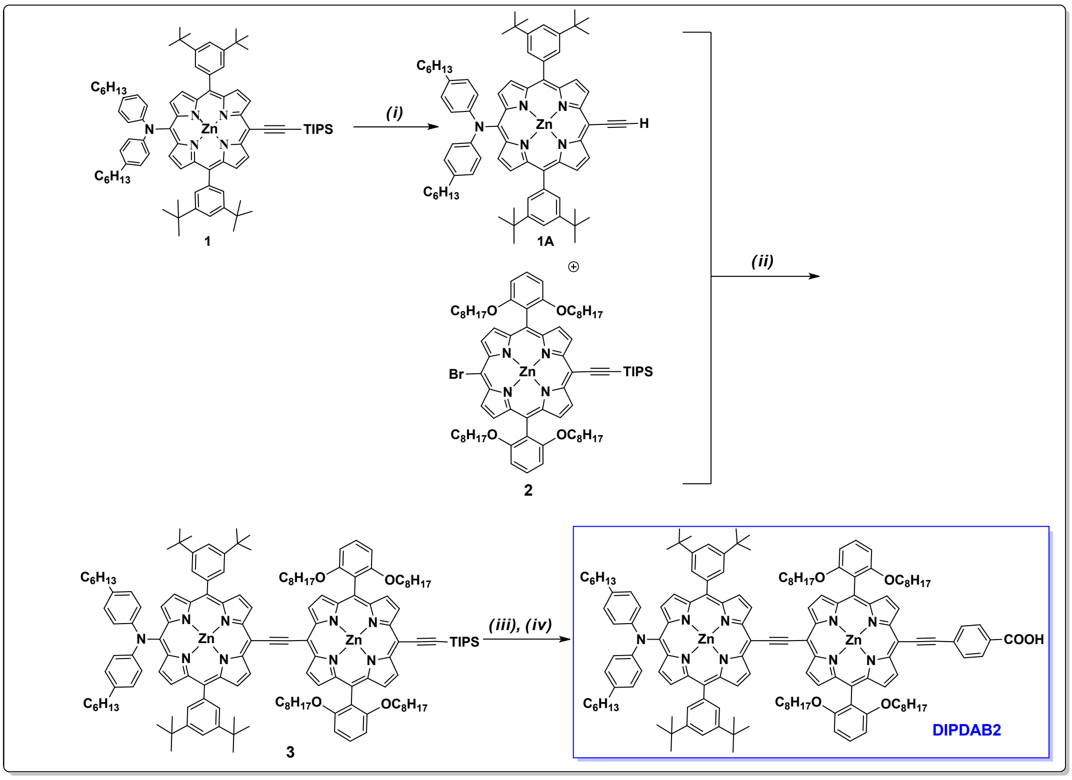

Fig. S3 Synthesis scheme of **DIPDAB2**: a new porphyrin dimer dye. The reactants are: (i) Tetra-n-butylammonium fluoride (TBAF), **tetrahydrofuran** (THF) (ii) Tris(dibenzylideneacetone)dipalladium(0)($Pd_2(dba)_3$), Triphenylarsine($AsPh_3$), THF/ Triethylamine (Et_3N), (iii) TBAF, THF (iv) $Pd_2(dba)_3$, $AsPh_3$, THF/Et_3N, 4-iodobenzoic acid.

DIPDAB2-TIPS (Compound 3). To a solution of the compound **1** (0.40 g, 0.32 mmol) in THF (30 mL), TBAF (0.3 mL, 0.3 mmol, 1 M solution in THF) was added at 0 ^{o}C. The mixture was stirred at 0 ^{o}C for 30 minutes. Then, the reaction was quenched with water, and extracted with dichloromethane (DCM, 30 mL) three times. The DCM solution of the extract was dehydrated using anhydrous Na_2SO_4 and the solvents were evaporated in vacuum to afford the residual compound **1A**, which was used in the next step without any further purification. The compound **1A** and compound **2** (0.68 g, 0.52 mmol) were dissolved in a mixture of THF (60 mL) and Et_3N (12 mL). Degassed $Pd_2(dba)_3$ (0.07 g, 0.072 mmol) and $AsPh_3$ (0.23 g, 0.72 mmol) were added to the solution to promote the reaction between the compound **1A** and compound **2**, and further degassed for 15 minutes. Then, the reaction mixture was refluxed for 5 h, followed by evaporation of the solvents in vacuum. The crude residue was purified using silica gel columns and Hexane:DCM (8:2) as an eluent to give brownish black solid, which was recrystallized using CH_3OH to give the pure compound **3** (0.40 g, 54.4 % yield). ^{1}H NMR spectrum is shown in Fig. S4: (400 MHz, $CDCl_3$, δ): 10.41 (d, *J* = 4.6 Hz, 2H; Por-H), 10.34 (d, *J* = 4.6 Hz, 2H; Por-H), 9.7 (d, *J* = 4.6 Hz, 2H; Por-H), 9.3 (d, *J* = 4.6 Hz, 2H; Por-H), 9.12 (d, *J* = 4.4 Hz, 2H; Por-H), 9.06 (d, *J* = 4.6 Hz, 2H; Por-H), 8.9 (d, *J* = 4.4 Hz, 2H; Por-H), 8.8 (d, *J* = 4.6 Hz, 2H; Por-H), 8.1 (d, *J* = 1.9 Hz, 4H; Ar-H), 7.8 (t, *J* = 1.7 Hz, 2H; Ar-H), 7.7 (t, *J* = 8.5 Hz, 2H; Ar-H), 7.28 (d, *J* = 8.2 Hz, 4H; Ar-H), 7.23 (d, *J* = 8.2 Hz, 4H; Ar-H), 7.01 (dd, *J* = 8.5 Hz, 8H; Ar-H), 3.87 (t, *J* = 6.5 Hz, 8H; O-CH$_2$), 2.49 (t, *J* = 7.8 Hz, 4H; Ar-CH$_2$), 1.55 (s, 36H; *ter*-CH$_3$), 1.51 (s, 21H; Si-CH&CH$_3$), 1.25 (m, 16H; CH$_2$), 1.03 (m, 8H; CH$_2$), 0.84 (t, *J* = 6.5 Hz, 6H; CH$_3$), 0.71 (m, 8H; CH$_2$), 0.52-0.42 (m, 32H; CH$_2$), 0.36 (t, *J* = 6.5 Hz, 12H; CH$_3$). MALDI-TOF-MS spectrum is shown in Fig. S5: m/z calcd for $C_{149}H_{187}N_9O_4SiZn_2$:2326.98, found: 2328 (M+1 100%).

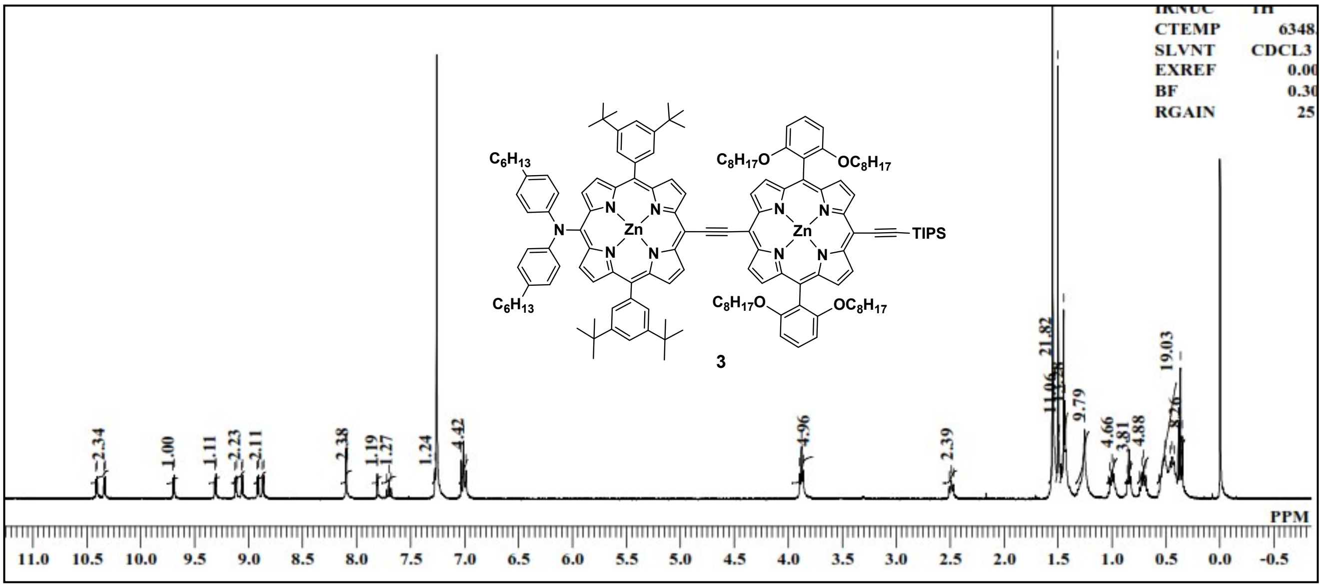

Fig. S4 ^{1}H NMR spectrum of the compound **3** ($CDCl_3$, 400MHz).

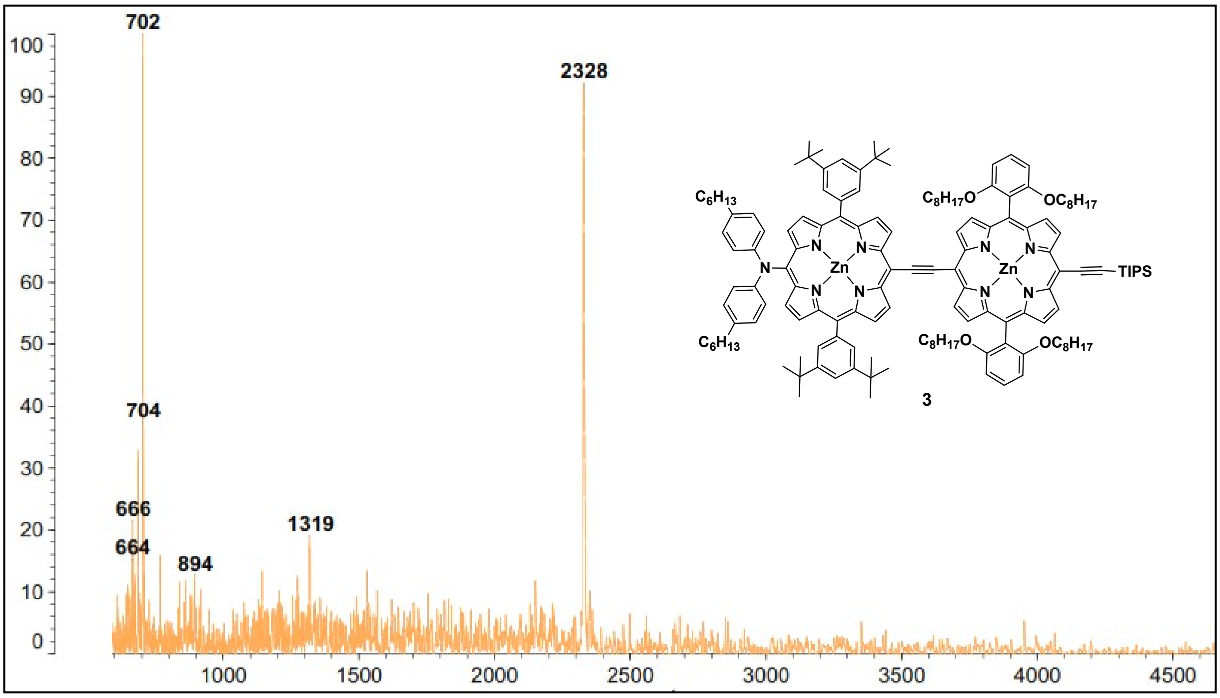

Fig. S5 MALDI-TOF-MS spectrum of the compound **3.**

DIPDAB2. To a solution of the compound **3** (0.2 g, 0.08 mmol) in THF (20 mL), TBAF (0.2 mL, 0.01 mmol 1 M in THF) was added at 0 °C. The mixture was stirred at 0 °C for 30 minutes. Then, the reaction was quenched with water, and then extracted with DCM (30 mL) three times. The DCM solution of the extract was dehydrated using anhydrous Na_2SO_4, and then the solvents was evaporated using a high vacuum rota vapour to obtain an intermediate product, which was used in the next step without any further purification. The crude product and 4-Iodo benzoic acid (0.21 g, 0.86 mmol) were dissolved in a mixture of THF (20 mL) and Et_3N (6 mL). The solution was degassed for 15 minutes. Degassed $Pd_2(dba)_3$ (0.02 g, 0.02 mmol) and $AsPh_3$ (0.053 g, 0.2 mmol) were added to the solution and refluxed for 5 hours. After the reaction was completed, the solvent was evaporated under reduced pressure. The resulting residue was purified using silica gel columns and DCM: CH_3OH (20:1) as a eluent to obtain a semi-solid, which was recrystallized with CH_3OH/Ether to give the title compound **DIPDAB2** (0.15 g, 76.1%) of a brownish black solid. ^1H NMR spectrum is shown in Fig. S6: (400 MHz , $CDCl_3$, δ): 10.41 (d, *J* = 4.5 Hz, 2H,Por-H), 10.35 (d, *J* = 4.5 Hz, 2H; Por-H), 9.7 (d, *J* = 4.5 Hz, 2H; Por-H), 9.31 (d, *J* = 4.6 Hz, 2H; Por-H), 9.13 (d, *J* = 4.5 Hz, 2H; Por-H), 9.07 (d, *J* = 4.5 Hz, 2H; Por-H), 8.96 (d, *J* = 4.5 Hz, 2H; Por-H), 8.87 (d, *J* = 4.6 Hz, 2H; Por-H), 8.23 (d, *J* = 7.8 Hz, 2H; Ar-H), 8.1 (d, *J* = 1.7 Hz, 4H, Ar-H), 8.07 (d, *J* = 7.8 Hz, 2H; Ar-H), 7.81 (t, *J* = 1.7 Hz, 2H; Ar-H), 7.73 (t, *J* = 8.4 Hz, 2H; Ar-H), 7.27 (d, *J* =8.2 Hz, 4H; Ar-H), 7.26 (d, *J* =8.2 Hz, 4H; Ar-H), 7.05 (d, *J* = 8.6 Hz, 4H; Ar-H), 6.98 (d, *J* = 8.6 Hz, 4H; Ar-H), 3.90 (t, *J* = 6.3 Hz, 8H; O-CH_2), 2.49 (t, *J* = 7.5 Hz, 4H; Ar-CH_2), 1.53 (s, 36H; *tert*-CH_3), 1.26 (m, 16H; CH_2), 1.03 (m, 8H; CH_2), 0.86 (t, *J* = 6.8 Hz, 6H; CH_3), 0.75 (m, 8H; CH_2), 0.55-0.46 (m, 32H; CH_2), 0.38 (t, *J* = 7.3 Hz, 12H; CH_3). FT-IR (KBr) spectrum is shown in Fig. S7: 2923 (Ar-C-H, O-H stretching), 2853 (Aliphatic-C-H stretching), 2360 (C≡C stretching), 2338 (Por-C≡C-Por stretching), 1699 (Ph-C=O stretching), 1649 (Ar-C=N stretching), 1572 (Ar-C=C stretching), 1538 (C-C stretching), 1433 (C-O stretching), 1338 (C-N stretching), 1315 (C-H bending), 1243 (C-O stretching), 1095 (C-N, C-H bending), 948 (C-C bending) cm^{-1}; UV-vis [0.01mM, in THF, λ_{max} (nm) & ε ($mol^{-1}cm^{-1}$)]**:** 421 (152,907), 445(166,502) , 458 (156,748), 491(316,864), 579(22,935) and 745(132,449). Elemental analysis: calc for $C_{147}H_{171}N_9O_6Zn_2 \cdot 2H_2O$ C 75.88 %, H 7.58 %,N 5.42 %; found C 75.80 %, H 7.47 %, N 5.23 %. MALDI-TOF-MS spectrum is shown in Fig. S8: *m/z* calcd for $C_{147}H_{171}N_9O_6Zn_2$: 2290, found: 2289 (M-1 100%).

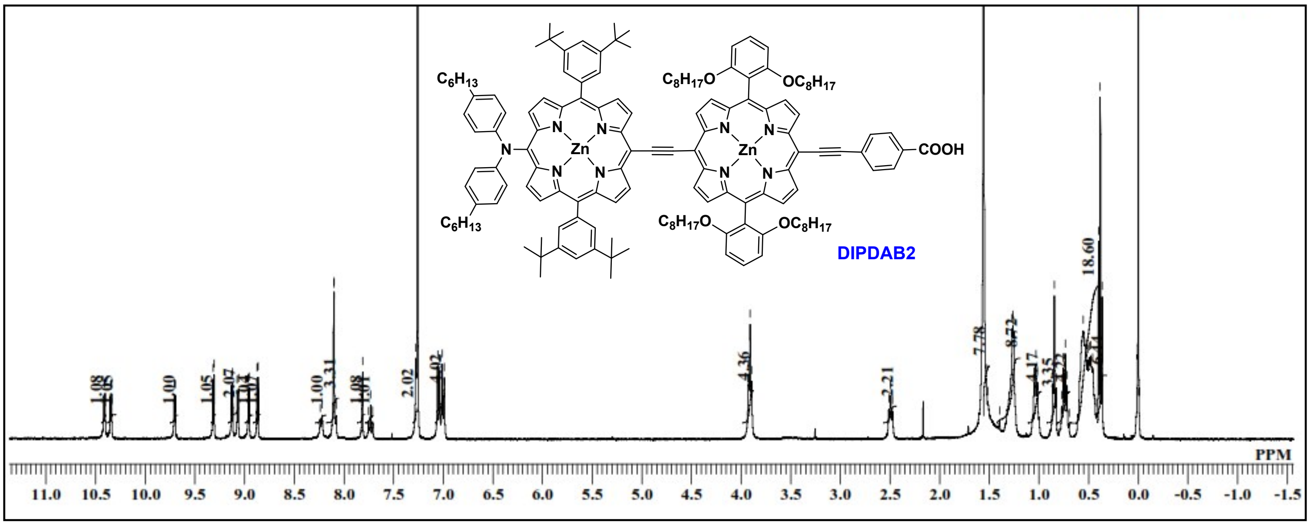

Fig. S6 ^{1}H NMR spectrum of **DIPDAB2** ($CDCl_3$, 400MHz).

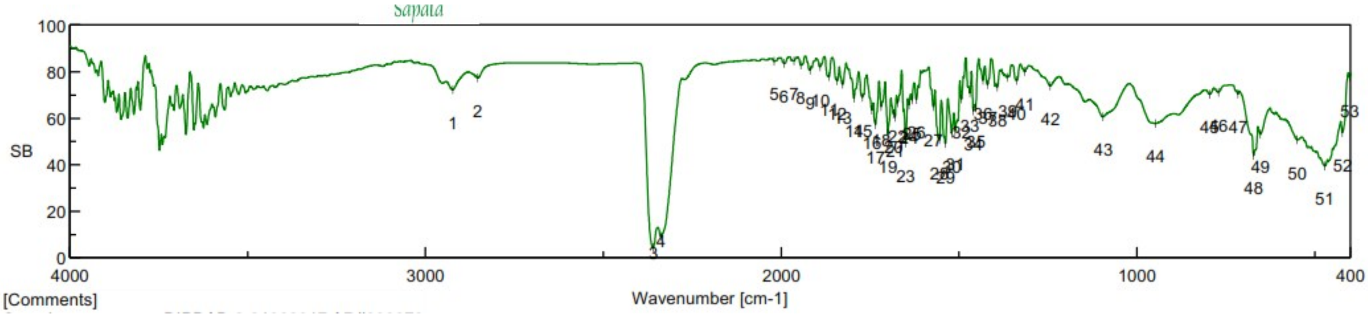

Fig. S7 FT-IR spectrum of **DIPDAB2.**

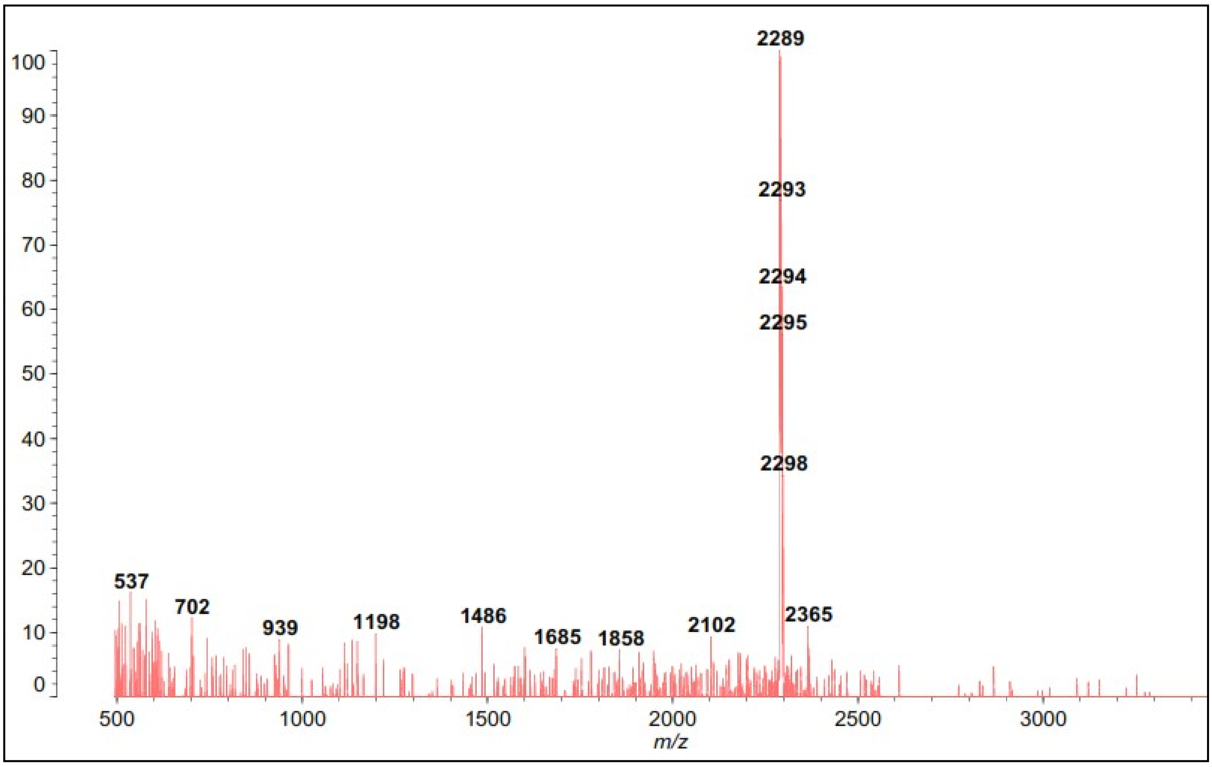

Fig. S8 MALDI-TOF-MS spectrum of **DIPDAB2.**

Co-sensitizers used with DIPDAB2

To achieve high absorbance in the whole of the visible−near-IR range, two kinds of organic dyes of D131 and D358 were used as co-sensitizers with DIPDAB2. The molecular structures of these two dyes are displayed in Fig. S9.

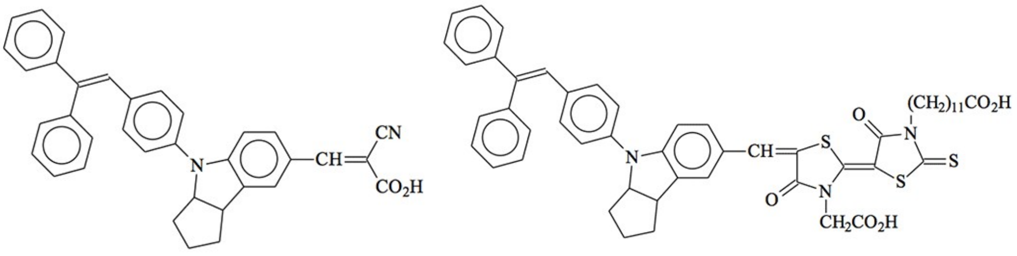

D131 (Yellow) D358 (Red)

Fig. S9 Molecular structures of **D131** and **D358.**

Evaluation of liquid electrolyte DSCs

Absorption properties of the four kinds of dyes and photovoltaic properties of the liquid electrolyte DSCs using these dyes are summarized in Table S1. **DIPDAB2** exhibits high performance comparable with that of **LDD1**.

Tabel S1 Absorption coefficients at the Q bands of the porphyrin dimers and photovoltaic parameters of the optimized liquid electrolyte DSCs using **DTBC, YDD6, LDD1** and **DIPDAB2** porphyrin dimer dyes. The data of **YDD6** and **LDD1** were quoted from Refs. 6 and 7, respectively.

Porphyrin dimer	*Absorption coefficents*	λ *max*	*Jsc*	*Voc*	*FF*	η
	/ 10^5 $M^{-1}cm^{-1}$	/ nm	/mA/cm^{-2}	/V		/%
DTBC	0.573	722	9.52±0.60	0.59±0.002	0.75±0.50	4.19±0.2
YDD6	0.85	741	9.66±0.84	0.67±0.002	0.724±0.60	4.7±0.2
LDD1	1.25	760	18.80	0.69	0.68	8.80
DIPDAB2 (This work)	1.33	745	18.6±0.2	0.65±0.1	0.65±0.1	7.7±0.15

Evaluation of SDSCs

An aperture mask of 0.196cm^2 was used to determine the irradiation area for evaluation of the photovoltaic performance of the SDSCs.

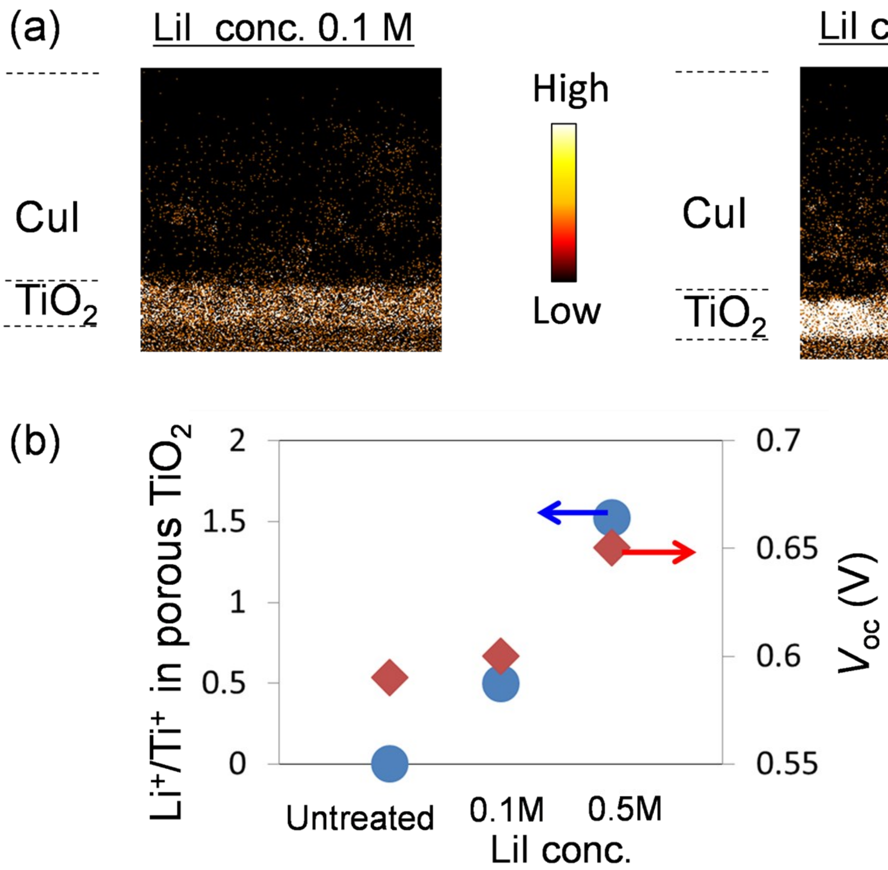

Fig. S10 (a) Time-of-flight secondary ion mass spectroscopy (TOF-SIMS) mapping of Li with different LiI concentrations. (b) Li$^+$/Ti$^+$ ratios in the porous TiO$_2$ electrodes and V_{oc} of the SDSCs.

Table S2 Photovoltaic parameters of the optimized SDSCs using the multi-dye (**DIPDAB2**+**D131**+**D358**) before/after the light soaking. The light soaking was conducted by irradiating AM1.5G 1sun light for 1 hour.

		Jsc	*Voc*	*FF*	*η*
	Cell number	/mA/cm^{-2}	/V		/%
Before light soaking	1	22.30	0.58	0.68	8.70
	2	22.77	0.54	0.66	8.11
	3	22.09	0.56	0.68	8.48
	4	22.05	0.58	0.68	8.72
	5	21.11	0.59	0.70	8.70
	6	22.80	0.58	0.66	8.72
	Average	22.19±0.60	0.57±0.018	0.68±0.016	8.57±0.26
After light soaking	1	22.00	0.65	0.71	10.09
	2	21.63	0.61	0.69	9.09
	3	21.58	0.63	0.69	9.36
	4	20.91	0.66	0.72	10.03
	5	19.50	0.68	0.71	9.42
	6	22.00	0.65	0.70	10.01
	Average	21.27±0.91	0.65±0.028	0.70±0.014	9.67±0.38

References

1. S. Moribe, A. Takeichi, J. Seki, N. Kato, K. Higuchi, K. Ueyama, K. Mizumoto, T. Toyoda, *Appl. Phys. Express*, 2012, **5**, 112302.
2. G. R. A. Kumara, A. Konno, K. Shiratsuchi, J. Tsukahara, K. Tennakone, *Chem. Mater*. 2002, **14**, 954.
3. S. Moribe, N. Kato, K. Higuchi, K. Mizumoto, T. Toyoda, *Appl. Phys. Express*, 2017, **10**, 042301.
4. M. Sreenivasu, A. Suzuki, Ch. V. Kumar, B. Sreekanth, S. Rajendar, D. Rambabu, R. Satish Kumar, P. Mallesham, N. V. Bhaskar Rao, M. Suresh Kumar and P. Y. Reddy, *Chemistry - A European Journal,* 2014, **20**, 14074-14083.
5. A. Yella, H. W. Lee, H. N. Tsao, C. Yi, A. K. Chandiran, M. K. Nazeeruddin E. W. G. Diau, C. Y. Yeh, S. M. Zakeeruddin, M. Gratzel, *Science,* 2011, **334**, 629-634.
6. H.-P. Wu, Z.-W. Ou, T.-Y. Pan, C.-M. Lan, W.-K. Huang, H.-W. Lee, N. M. Reddy, C.-T. Chen, W.-S. Chao, C.-Y. Yeh, E.W.-G. Diau, *Energy Environ. Sci.,* 2012, **5**, 9843.
7. J.-W. Shiu, Y. -C. Chang, C. -Y. Chan, H.-P. Wu, H.-Y. Hsu, C.-L. Wang, C.-Y. Lin, E.W.-G.Diau, *J. Mater. Chem.A.*,2015, **3**, 1417.